Chapter 1

Biopolymeric Nanoparticle Synthesis in Ionic Liquids

Mercedes G. Montalbán, Guzmán Carissimi, A. Abel Lozano-Pérez, José Luis Cenis, Jeannine M. Coburn, David L. Kaplan and Gloria Víllora

Additional information is available at the end of the chapter

http://dx.doi.org/10.5772/intechopen.78766

Abstract

Recently, much research has focused on the use of biopolymers, which are regarded as biodegradable, natural, and environmentally friendly materials. In this context, biopolymeric nanoparticles have attracted great attention in the last few years due to their multiple applications especially in the field of biomedicine. Ionic liquids have emerged as promising solvents for use in a wide variety of chemical and biochemical processes for their extraordinary properties, which include negligible vapor pressure, high thermal and chemical stability, lower toxicity than conventional organic solvents, and the possibility of tuning their physical–chemical properties by choosing the appropriate cation and anion. We here review the published works concerning the synthesis of biopolymeric nanoparticles using ionic liquids, such as trimethylsilyl cellulose or silk fibroin. We also mention our recent studies describing how high-power ultrasounds are capable of enhancing the dissolution process of silk proteins in ionic liquids and how silk fibroin nanoparticles can be directly obtained from the silk fibroin/ionic liquid solution by rapid desolvation in polar organic solvents. As an example, their potential biomedical application of curcumin-loaded silk fibroin nanoparticles for cancer therapy is also discussed.

Keywords: ionic liquid, biopolymer, nanoparticle, synthesis, silk fibroin

1. Introduction

1.1. Biopolymeric nanoparticles for biomedical applications

During the last 30 years, nanotechnology has attracted much attention in many engineering fields including electronic, mechanical, biomedical, and space engineering. Among these fields,

nanotechnology has led to significant progress being made in biomedicine through the development of efficient structures for controlled and targeted drug or gene delivery, tissue engineering, the imaging of specific sites, regenerative medicine, biosensing, and probing of the DNA structure [1]. More specifically, the role of nanoparticles in the progress made in this field is of particular note, and treatments involving nanoparticles have been widely applied in cancer therapy, diabetes, allergy, infection, and inflammation [2]. The main advantages of *nanoparticles* used as drug carriers for the treatment of these diseases are the following: (a) a size range similar to that of proteins, (b) a large surface area, which allows the presence of different functional groups acting as ligands, (c) fast absorption and release properties, and (d) particle sizes and surface features that can be specifically designed.

Nanoparticles for therapeutic application can be synthesized from (natural or synthetic) polymers, ceramics, and metals [3]. Polymeric nanoparticles have been widely studied as nanocarriers of active molecules such as drugs and genes [4–9]. The main drawbacks in the use of polymeric nanoparticles are the difficulty of scaling up, and their low drug loading capacity and wide size distribution [2]. However, as nanoplatforms, they show great potential because they allow the targeted release of drugs to specific cells or tissues [10]. Moreover, in contrast to ceramic or metal nanoparticles, polymeric nanoparticles can be synthesized in a wide range of sizes and forms and can sustain localized drug therapeutic agents for weeks [3]. While the above features are common to both natural and synthetic polymers, natural polymers, also known as biopolymers, have some extra advantages such as their inherent biocompatibility and biodegradability, non-antigenicity, a high nutritional value, the abundance of their renewable sources, and an extraordinary binding capacity with several drugs [11]. Biopolymers are natural macromolecules and can be polysaccharides, proteins, polyphenols, polyesters, or polyamides. The synthesis of biopolymer-based materials, such as nanoparticles, is still difficult due to the low solubility of biopolymers in conventional organic solvents as a result of their highly crystalline structure [1]. Therefore, the search for new solvents capable of dissolving biopolymers successfully is a continuous challenge in order to achieve the industrial fabrication of biomaterials.

1.2. Ionic liquids as media for the synthesis of nanoparticles

Ionic liquids (ILs) are organic salts that are liquid close to room temperature. They normally consist of an organic cation and a polyatomic inorganic anion. They have attracted great attention recently for use in a variety of chemical processes as “green” solvents. The most important advantage of ILs is their non-detectable vapor pressure, which makes them environmentally benign solvents compared with volatile organic solvents (VOSs). The growing awareness about the risk of using these solvents has led to a search for alternatives, and the discovery of ILs seemed to solve the problem [12]. They also show several advantages over classic organic solvents such as a good chemical and thermal stability, a high ionic conductivity, non-flammability, a large electrochemical window, solvation ability, and they can be used at high temperatures [13, 14]. Furthermore, the physical–chemical properties of ILs, such as their density, polarity, hydrophobicity, melting point, viscosity, and solvent properties, may be tuned by modifying the anion or the cation. Among other applications, ILs have been used as electrolytes, solvents, lubricants, matrices for mass spectrometry, for chromatography as

stationary phase, supports for the enzyme immobilization, as liquid crystals, in technologies of separation, for nanomaterials synthesis as templates, in the synthesis of catalytic membranes, and in the generation of high conductivity materials [13, 14].

ILs may be excellent candidates for dissolving biopolymers and developing biomaterials mainly because of the flexibility that can be achieved by combining different cations and anions, and green solvent properties such as non-volatility, non-flammability, and recyclability. During recent years, biopolymers such as cellulose, xylan, starch, chitin/chitosan, keratin, silk fibroin (SF), and heparin have been transformed from ILs into films, scaffolds, membranes, fibers, and micro- or nanoparticles. In addition, composites formed by biopolymer/biopolymer or biopolymer/synthetic polymer mixtures can also be synthesized by the co-dissolution of polymers in ILs [1]. The interesting properties of ILs make them excellent media for the synthesis and stabilization of nanoparticles [15]. Their most noteworthy features for the synthesis of nanoparticles are as follows:

a. ILs can contribute to the synthesis of small particles due to their generally low surface tension, which leads to high nucleation rates.

b. ILs enhance the electronic and steric stabilization of nanoparticles and reduce particle growth, since their constituents (anion and cation) form a protective electrostatic shell that prevents agglomeration processes. In addition, nanoparticles are stable in solution due to the coordination of anion or cation through ionic or covalent bonds.

c. ILs have a significant effect on the shape of the synthesized nanoparticles because they are highly structured liquids which can form extended hydrogen-bonded networks.

d. ILs can be designed using different cation/anion combinations to achieve the desired properties of density, viscosity, hydrophilicity, gas solubility, and so on.

e. ILs can act as reactive agents, which may be of interest for the synthesis of nanoparticles by chemical reactions.

f. The choice of IL used for the synthesis of nanoparticles determines, at least partially, their properties, including water solubility.

g. ILs possess negligible vapor pressure and are non-flammable, which allows safer operation at high temperature and under vacuum than with conventional organic solvents.

h. ILs can be tailored following the 12 principles of green chemistry developed by Anastas and Warner [16] which, besides non-volatility, low toxicity, non-corrosiveness, and non-flammability, do not include requiring auxiliary or separation solvents.

In short, the synthesis of nanoparticles using ILs can be carried out by the following procedures that are more environmentally friendly than those using conventional organic solvents.

In this chapter, the processes used to synthesize biopolymer (polysaccharide or protein) nanoparticles using ILs are reviewed. To the best of our knowledge, the biopolymers used to obtain nanoparticles in processes involving ILs are cellulose, xylan, starch, chitosan, keratin, and silk fibroin. A previous work of the authors based on the synthesis of silk fibroin nanoparticles by dissolving the protein in several ILs is discussed. An example of the biomedical application of curcumin-loaded silk fibroin nanoparticles obtained with this method is also shown.

1.3. Methods of synthesis

One method used to obtain nanoparticles in ILs is synthesis *via* physical vapor deposition (PVP) since, due to the negligible vapor pressure of most ILs, they can be manipulated under high vacuum conditions even at high temperatures [17]. This method has been used to obtain metal nanoparticles through vaporization of a metal, an intermetallic phase, or a metal salt in the presence of an IL, for example, copper nanoparticles in the IL butyl-3-methylimidazolium hexafluorophosphate, [bmim$^+$][PF_6^-]. By means of this technique, metal nanoparticles can be deposited not only on the IL but also onto materials dispersed in the IL, as occurs in the formation of Cu/ZnO nanocomposites in butyl-3-methylimidazolium bis{(trifluoromethyl)sulfonyl}imide, [bmim$^+$][NTf_2^-]. Nevertheless, to our knowledge, the PVP method has never been applied to obtain nanoparticles from biopolymers in ILs.

Microwave synthesis may be used to profit from the presence of large ions with high polarizability and conductivity of the ILs, which makes them very good media for absorbing microwaves, leading to high heating rates that result in the rapid formation of nuclei (nanoparticles) [18, 19]. Control over the particle size range can be achieved by changing the process temperature and time, as well as reactant concentrations and the choice of the anion and cation constituents of the IL. If the heat spreads uniformly through the sample, a narrow nanoparticle size distribution may be obtained. As an example, silver and gold nanoparticles have been obtained by microwave synthesis in 2-hydroxyethyl-N,N,N-trimethylammonium bis{(trifluoromethyl)sulfonyl}amide. Swatloski et al. [20] used microwave heating on a [bmim$^+$][Cl^-]/cellulose solution to dissolve cellulose, but they did not analyze cellulose degradation. Phillips et al. [21] tried to dissolve silk fibroin in [bmim$^+$][Cl^-] using a domestic microwave but were unsuccessful due to the thermal decomposition of the silk. However, our group has found that, by using a laboratory microwave with a strict control of the temperature and time, the integrity of the protein is preserved and nanoparticles can be obtained from silk fibroin-IL solutions by precipitation in polar organic solvents.

Ultrasound synthesis is another alternative that can be used as energy source for the preparation of many materials such as metal, oxide, sulfide, and carbide nanoparticles, and the use of ultrasound power has recently become popular in combination with ILs as the reaction medium [22]. We used high-power ultrasounds to enhance the dissolution process of silk proteins in ILs to obtain silk fibroin nanoparticles (SFNs) directly from the silk/ionic liquid solution (SIL) by rapid desolvation in polar organic solvents [23].

2. Synthesis of biopolymer nanoparticles using ILs

2.1. Cellulose

Cellulose is the main constituent of the vegetal kingdom and brown algae, making it the most abundant polysaccharide on earth. It plays a structural role in the cell wall and other surface structures of some amoebae, alveolates, chromists, and red and green algae. The molecular structure of this biopolymer is composed of D-glucopyranose units linked together by a β(1➔4)

glyosidic bond to form a linear structure. The degree of polymerization (DP) varies from the source but can be as high as 23,000 units. Cellulose has a ribbon-like structure, with two units per turn of 1.03 nm, dictated by the allowed angles of C_1-O and O-C_4 [24, 25]. In terms of density (1.5 Mgm^{-3}), cellulose fibers are stiffer (Young's modulus 50–130 GPa) and stronger (1 GPa), when measured along the polymer length, than nylon, silk, chitin, collagen, tendon, or bone [26]. Cellulose is completely insoluble in water, mainly because its hydrogen-bonding capabilities are occupied by side chains, forming aggregates. Nevertheless, it has been demonstrated that the IL 1-butyl-3-methylimidazolium chloride ([$bmim^+$][Cl^-]) is able to solubilize cellulose even at high DP (6500 units), making it an appropriate reaction medium [24]. A review of the solubility of cellulose in ILs is provided by Lee et al. [1].

Swatloski et al. [20] carried out experiments using cellulose-dissolving pulps, fibrous cellulose, and Whatman cellulose filter papers. They prepared the cellulose solutions by the addition of the cellulose to the ionic liquids without pretreatment and heated on a heating plate or in a domestic microwave oven. These authors were able to dissolve 25 wt% cellulose in [$bmim^+$][Cl^-] using microwave heating. Nevertheless, ILs containing "non-coordinating" anions, including [BF_4]- and [PF_6]-, were nonsolvents, presumably because cellulose solubilizes through hydrogen bonding from hydroxyl functions to the anions of the solvent, [Cl^-]. The authors did not analyze the peak temperature reached during the microwave dissolution step nor the extent of cellulose degradation.

Han et al. [27] synthetized cellulose nanoparticles by dissolving microcrystalline cellulose (MCC) or cotton cellulose (CC) in [$bmim^+$][Cl^-]. The preparation of cellulose nanoparticles involves four steps: dissolution, regeneration, homogenization, and freeze-drying. Before proceeding to the dissolution process, solid state [$bmim^+$][Cl^-], MCC, or CC have to be vacuum-dried to remove the remnants of water, whose presence can significantly impair cellulose solubility in IL by competing with the IL for hydrogen bonds to the cellulose microfibrils [20]. Then, the cellulose was dissolved in IL, using a magnetic hot plate stirrer with safety control, by stirring the 5% w/w disperse fibers for 5 h in a 125°C oil bath. When a clear phase was obtained, the solution was slowly poured into distilled water and a white dispersion of nanoparticles immediately appeared. In order to remove IL, the dispersion was filtered, centrifuged, washed three times, and, eventually, dialyzed. To further enhance the suspension, the sample was run through a high-pressure homogenization, and, finally, the suspensions were quickly frozen by mixing acetone and dry ice in an ice pot and transferred to a freeze-dryer. Particles regenerated from MCC yield rods of 112 ± 42 nm in length with an aspect ratio of 9.21 (**Figure 1c**) and spherical nanoparticles with a diameter of 118 ± 32 nm (**Figure 1e** and **f**). Particles regenerated from CC formed only nanorods of 123 ± 34 nm with an aspect ratio of 9.96 (**Figure 1d**).

When infrared spectra were used to characterize the cellulose structure of samples, structural changes from a cellulose crystalline structure I to II were evident. For instance, after the regeneration of cotton cellulose, the -CH stretching vibration signals moved from 2901 to a lower 2893 cm^{-1}, the CO stretching vibration at C-6 switched from 1033 to 1025 cm^{-1}, and COC vibration from β-glycosidic linkage shifted from 897 to 894 cm^{-1}, probably due to changes in glycosidic linkage torsion angles. For both the MCC and MCC-NP, spectra showed strong

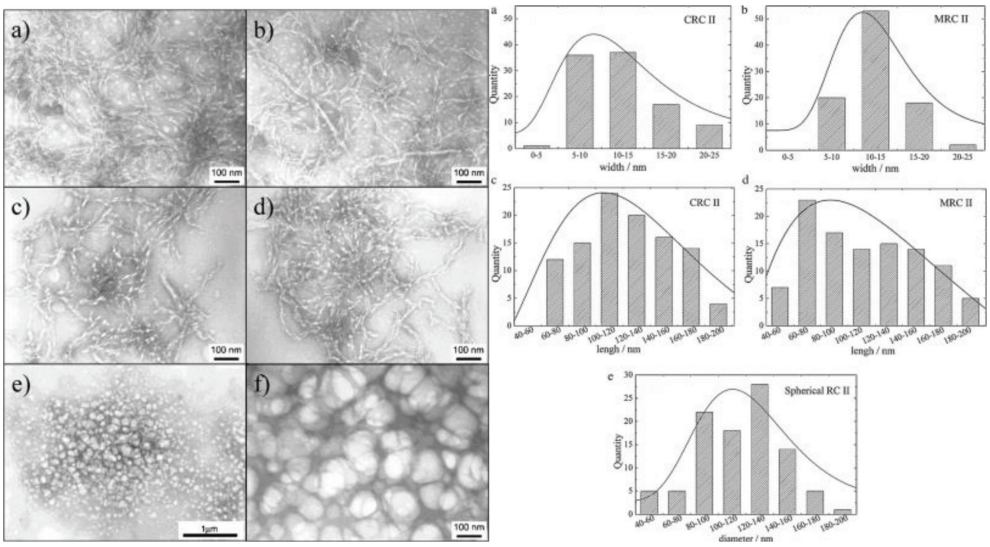

Figure 1. (Left) TEM images of MCC-NP (a), CC-NP (b), homogenized MCC-NP (c), homogenized CC-NP (d), and spherical NP from MCC (e, f). (Right) The dimension distribution of homogenized CC-NP, MCC-NP, and spherical MCC-NP. (a) and (b) width distribution of C-RCNs and M-RCNs; (c) and (d) length distribution of C-RCNs and M-RCNs; (e) diameter distribution of spherical RCNs. From Ref. [27] with permission of Elsevier Limited.

hydrogen bonded OH stretching vibrations in the range of 3000–3600 cm^{-1}. The signals at around 1430 and 2900 cm^{-1} were awarded to CH_2 (C6) bending vibration and CH stretching vibration, respectively. Adsorbed water was noticed by a peak at 1644 cm^{-1} from O-H bending. Characteristic FTIR absorption bands related to the transition from cellulose I to cellulose II were also watched. A deeper analysis of the structural changes can be found in the author's publication [27] and references therein. The lack of absorption bands from [$bmim^+$][Cl^-] suggests that the ILs were successfully removed. The properties of regenerated cellulose nanoparticles produced from microcrystalline cellulose and cotton using a combined IL and high-pressure homogenization treatment point to the potential for application in the biomedicine field as drug delivery systems, biomarkers, tablet excipients, and more (**Figure 2**).

Cellulose is susceptible to modification due to its hydroxyl groups; for example, silylation is one possible route for the synthesis of water-soluble derivatives, thus broadening the spectrum of possibilities. Silylation can take place in heterogeneous media like pyridine, or in homogeneous media, like methyl sulfoxide/LiCl. Nevertheless, in heterogeneous media, the reaction is not even at whole cellulose molecule and the use of homogeneous media is not applicable on a large scale as it is impossible to regenerate the media. Heinz's research group [28] prepared trimethylsilyl cellulose (TMSC) nanoparticles by taking advantage of the solubilizing power of IL and the self-assembly capabilities of TMSC. In brief, cellulose is first solubilized in [$emim^+$][Ac^-] 10% w/w, and hexamethyldisilane is added in a 3–1 excess molar ration with respect to the glucose units of cellulose. After a reaction time of 1 h at 80°C, a 2.65° of substitution (DS) was obtained. TMSC nanoparticles are dissolved in an organic solvent such as tetrahydrofuran

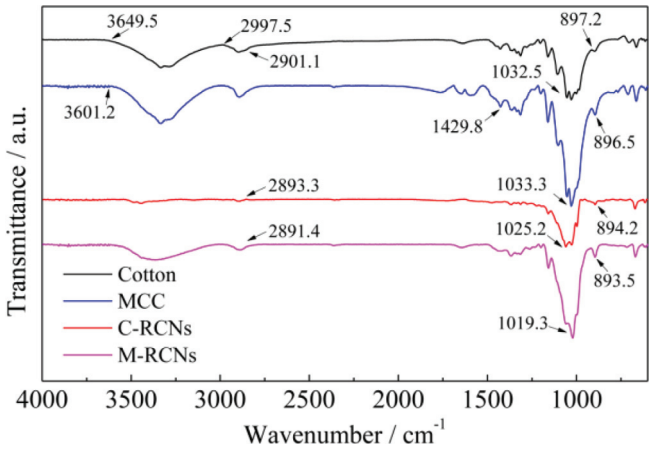

Figure 2. FTIR spectra of raw cotton, C-RCNs, untreated MCC and M-RCNs. From Ref. [27] with permission of Elsevier Limited.

or dimethyl acetone and dialyzed against water. Nanoparticles of 170 nm are formed based on the slow exchange of an organic solvent against an anti-solvent (non-solvent).

Cellulose-magnetite composites have also been prepared by suspension and dispersion of particles of magnetite in a homogeneous solution of cellulose in IL followed by regeneration in water and the subsequent preparation of films, flocs, fibers, or beads. The materials prepared were ferromagnetic, with a small superparamagnetic response. Characterization by X-ray diffraction showed that the initial magnetite was chemically unaltered after encapsulation, with an average particle size of approximately 25 nm [29].

2.2. Xylan

Xylan is the second most abundant polysaccharide in the vegetal kingdom after cellulose. It is the major component of hemicellulose, constituting 25–35% of the biomass of woody tissues of dicots and lignified tissues of monocots and up to 50% of some tissues of cereal grains [30]. It has a linear backbone constituted by β-D-xylosa units bound together by a β(1➔4) glyosidic bond. Xylan normally presents side chain sugars such as 4-O-methyl-glucuronic acid, galacturonic acid, and arabinose.

Gerick et al. [31] synthetized nanoparticles with a hydrodynamic radius of ca. 160 nm (**Figure 3**) of modified xylan with phenyl carbonate groups (DS up to 2.0). For the synthesis of xylan nanoparticles, 2 g of xylan and 18 g [$bmim^+$][Cl^-] were stirred for 1 h at 80°C. Afterwards, 5 mL of pyridine was added and stirred for 18 h at 80°C. The solution was cooled to 25°C under nitrogen atmosphere; then 15 mL of pyridine followed by 3.82 mL of phenyl chloroformate (60.8 mmol) were added. After 3 h of reaction time at 25°C, the mixture was poured into 300 mL ice cold water. The precipitate was removed by filtration and washed twice with 150 mL of water and twice with 150 mL of ethanol. The crude product was dissolved in 40 mL of DMSO

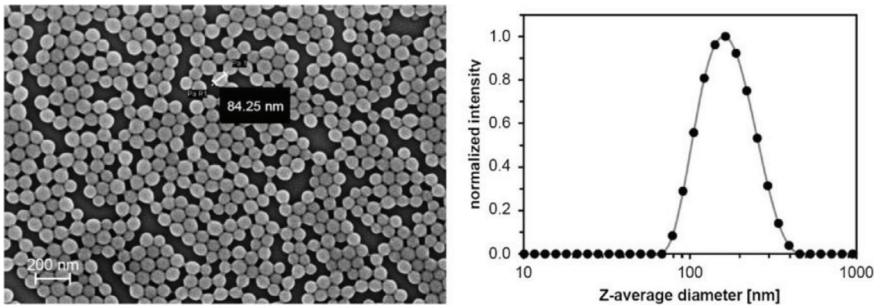

Figure 3. (left) Scanning electron microscopy images of nanoparticles obtained by dialysis of xylan phenyl carbonate XPC 20. (right) Size distribution of XPC 20 nanoparticles obtained by dynamic light scattering. From Ref. [31] with permission of Elsevier Limited.

and then precipitated in 300 mL of ethanol. This functionalization allows the molecule to have a major electrophilic center for further functionalization with drugs, signaling molecules, recognition molecules, and so on. Many other xylan modifications/functionalizations are described in Petzold-Welcke's review [32]. For example, the modification of xylan with a methyl group can be used as polymeric tensides, and some esters showed good drug-carrying capabilities. Xylan sulfate may be applied as antiviral drugs and as blood coagulation inhibitor.

2.3. Starch

Starch is produced by green plants to store energy. Granules of starch accumulate at high concentrations in reproductive structures like cereal grains (e.g., wheat, rice, maize, barley, rye, oats, millet, and sorghum) and in vegetative structures such as tubers (potatoes) and roots (cassava and taro) [33]. The two major forms of starch are amylose and amylopectin. The first is the liner polymer of D-glucopyranose units bound by α(1➔4) glyosidic bond. Its molecular weight varies from 10^4 to 10^5 with a DP of 250–1000 units. The second is a highly branched polymer of α(1➔4) glyosidic bonds and lateral chains of α(1➔6) with a molecular weight of 10^6–10^8, corresponding to a DP of 5000–50,000 units [34, 35].

Zhou et al. [36, 37] prepared starch nanoparticles with a controlled mean diameter of 64–255 nm with a water/ionic liquid emulsion (W/IL) cross-linked technique. To prepare the aqueous phase, 0.5 g of acid-treated granular starch was dissolved in 9.5 g of NaOH solution (20 M) and then added to 40 g of [$bmim^+$][PF_6^-] to form the water/IL microemulsion with 40 g of a mixture of TX-100 surfactant and 1-butanol cosurfactant (TX-100/1-butanol = 3:1, w/w) After several minutes of stirring, 1.84 of epichlorohydrin was added to the above microemulsion as a cross-linker. At this point, the mixture was stirred at 50°C for 4 h. Next, this solution was allowed to reach room temperature and methanol was used as antisolvent to precipitate the starch nanoparticles. The precipitate was centrifuged and washed thoroughly with sufficient methanol and ethanol to eliminate unreacted epichlorohydrin, remaining [$bmim^+$][PF_6^-], TX-100, and 1-butanol. Finally, the solid was dried in a vacuum for 24 h at 45°C. More examples of starch nanoparticle synthesis in IL emulsions can be found in the

study [38–40]. The drug-loading and -releasing capabilities of the starch nanoparticles were tasted with mitoxantrone hydrochloride.

2.4. Chitosan

Chitosan is a lineal polysaccharide constituted by randomly distributed β-(1 → 4)-linked D-glucosamine and N-acetyl-D-glucosamine. Chitosan is obtained from the deacetylation of chitin via basic hydrolysis. Chitin is mostly present in the exoskeleton of crustaceans, insect wings, and cell walls of fungi and algae, among others. Chitosan nanoparticles are widely used in food and bioengineering industries for the encapsulation of active food ingredients, enzyme immobilization, as a carrier for controlled drug delivery, and in agriculture as a plant antimicrobial agent and growth promoter [41]. For instance, Torzsas et al. showed that chitosan may have an important role in protecting against colon cancer [42] (**Figure 4**).

Bharmoria et al. [43] reported the synthesis of chitosan nanoparticles by ionic cross-linking with IL for the first time. The simple, self-assembling methods consist of adding [bmim$^+$][$C_8OSO_3^-$] or [omim$^+$][Cl^-] above the critical micelle concentration to an aqueous solution of chitosan. The chitosan chains are attracted to IL micelles by charge interactions and aggregate in a gelated complex. Acetone is used as antisolvent to precipitate the nanoparticles, which have a mean hydrodynamic diameter in the range of 300–560 nm with Z potential above +58.5 mV, depending on the IL used. The authors assumed that the electrostatic and hydrophobic interaction produced between chitosan and IL directs the formation of chitosan nanoparticle, where IL aggregates act as templates. Scanning electron microscopy (SEM) revealed that the nanoparticles obtained from chitosan-[bmim$^+$][$C_8OSO_3^-$] solutions have a greater sphericity and a lower tendency to agglomerate (**Figure 5**).

Chitosan nanoparticles have previously been tested for cellular uptake and trafficking to lymph nodes with very promising results [44]. Furthermore, chitosan-based nanoparticles are of special interest for the oral administration of insulin, as subcutaneous administration suffers disadvantages such as patient noncompliance and occasional hypoglycemia. Moreover, these last approaches do not mimic the normal physiological pattern of insulin release [45].

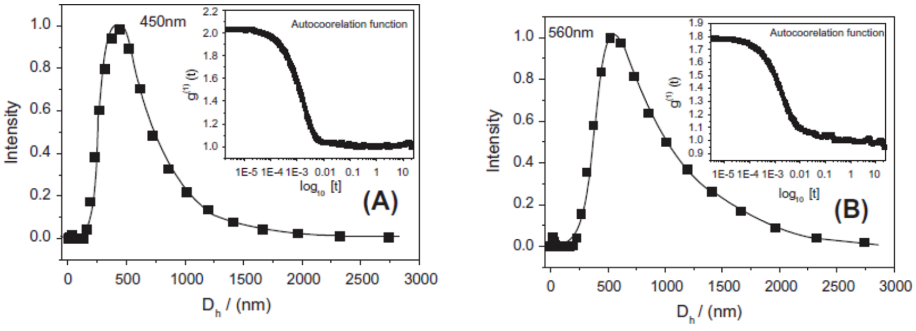

Figure 4. Hydrodynamic diameter (Dh) plots of chitosan nanoparticles formed with (A) [bmim$^+$][$C_8OSO_3^-$] and (B) [omim$^+$][Cl^-]. From Ref. [43] with permission of Elsevier Limited.

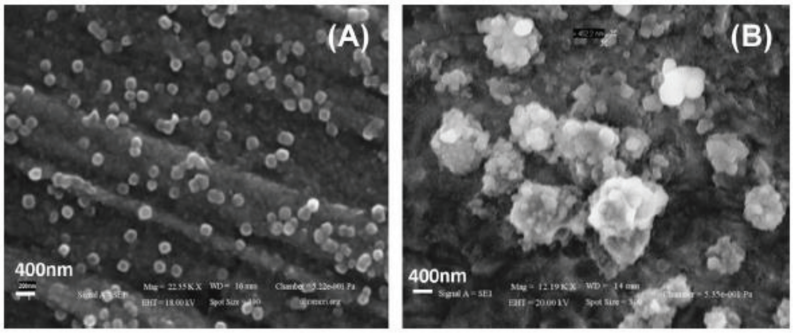

Figure 5. SEM images of nanoparticles formed with (A) [bmim$^+$][$C_8OSO_3^-$] and (B) [omim$^+$][Cl^-]. From Ref. [43] with permission of Elsevier Limited.

2.5. Silk fibroin

Due to its excellent biocompatibility and mechanical properties, silk fibroin (SF) obtained from *Bombyx mori* cocoons is an attractive biomaterial for use in biomedical and tissue engineering applications [46]. This biomaterial, formulated as particles, has potential applications in medicine for its capacity to adsorb, transport, and deliver a wide range of bioactive molecules [47]. Silks are insoluble in most solvents, including water, dilute acid, and alkali. There are two classical solvent systems to dissolve SF: *ionic hydro-alcoholic solutions*, such as a $CaCl_2$/ethanol/water mixture (Ajisawa's reagent) [48], or *ionic aqueous solutions*, traditionally 9.3 M LiBr or 50 wt% $CaCl_2$ solution [49]. These solutions require to be dialyzed for 48 h against ultra-pure water using a cellulose semi-permeable membrane (cut-off 3.5 KD) to remove salts, pigments, small peptides, and other impurities of the silk solution. Both processes are time-consuming, and the solutions are unstable and aggregate to a gel state. For long-term storage, aqueous solutions of SF can be lyophilized and redissolved in organic solvents such as 1,1,1,3,3,3-hexafluoroisopropanol (HFIP). However, these solvents are toxic and extremely corrosive, requiring considerable care in handling [50].

The suitability of imidazolium-based ionic liquid solvents, such as 1-butyl-3-methylimidazolium chloride ([bmim$^+$][Cl^-]), to form stable SF solutions was demonstrated [21]. Within an ionic liquid, the anion plays a larger role in dictating the ultimate solubility of the SF, attributed to the ability of the anion to disrupt the hydrogen bonding in the β-sheets of the silkworm SF to form solutions (mainly halogens or small carboxylates) [51]. The use of ILs as solvents has the advantage that the total number of steps required for the dissolution process is reduced and, furthermore, the cocoon can be dissolved directly because sericin was also dissolved in the selected ILs. However, complete dissolution of SF using the classic above-described methods takes several hours, even with intense heating at 100°C [21], resulting in the loss of protein integrity. Long treatments lead to breakage of the peptidic chains and poor mechanical properties of the resulting biomaterials. On the other hand, the process of silk dissolution may be improved by applying high-power ultrasounds to the SIL mixture to accelerate the process and by adding water to reduce the viscosity. High-power ultrasounds

have two important synergistic effects on the mixture: rapid heating and efficient disruption of the fibers at the same time. By applying the precipitation method commonly used for the coagulation of an aqueous SF solution in a water-miscible organic solvent, it is possible to obtain particles of regenerated SF [52].

The dissolution of *B. mori* SF using an oil bath as the heat source was investigated in the assembled state of the fibers. **Table 1** summarizes the results. Complete dissolution took over 1 h at 100°C, as described by Phillips et al. [21]. The saturated solubilities by weight for SF in 1-alkyl-3-methylimidazolium chlorides are dependent on the length of the alkyl substituent of the imidazolium ring.

It was checked that 1-alkyl-3-methyl imidazolium chlorides are able to disrupt the hydrogen bonding in silkworm SF and they are good solvents for silk dissolution when the length of the alkyl chain is lower than eight carbons [21]. The hydrophobicity of the organic cation increases with the cation alkyl chain length, so that long-aliphatic-chain ILs cannot dissolve SF. Likewise, ILs with highly hydrophobic anions cannot act as solvents of SF.

Silk proteins were successfully dissolved in the 1-alkyl-3-methylimidazolium chlorides (where 1-*alkyl* is: *methyl* [mim^+][Cl^-]; *ethyl* [$emim^+$][Cl^-]; *propyl* [$pmim^+$][Cl^-]; *butyl* [$bmim^+$][Cl^-] or *hexyl* [$hmim^+$][Cl^-]) using high-power ultrasounds and limiting the temperature at 100°C. The saturated solubility by weight and the time required for silk dissolution in selected ILs are listed in **Table 2**.

In an oil bath at 100°C, the thermal heating process of SF or SC dissolution in ILs takes hours, but instead, by using ultrasounds, a significant reduction is achieved in the time necessary to complete dissolution. The break of the β-sheet hydrogen bonds network of the proteins was enhanced by the use of the high-power ultrasounds.

Although the solubility of SF was highest in [$emim^+$][Cl^-], for particle formation, it is not necessary to reach a concentration higher than 10% (w/w), since an increased viscosity represents a handicap for handling.

IL	SF solubility (wt%)	IL	SF solubility (wt%)
[mim^+][Cl^-]	Soluble (>12%)	[eim^+][Cl^-]	Insoluble*
[$emim^+$][Cl^-]	Soluble (>23%)	[$emim^+$]$EtSO_4^-$	Insoluble*
[$pmim^+$] [Cl^-]	Soluble (>15%)	[$emim^+$]TfO^-	Insoluble*
[$bmim^+$][Cl^-]	Soluble (>12%)	[$bmim^+$]$OctSO_4^-$	Insoluble*
[$hmim^+$][Cl^-]	Soluble (>11%)	[$bBmim^+$]PF_6^-	Insoluble*
[$omim^+$][Cl^-]	Insoluble*	[3-MEP^+]$EtSO_4^-$	Insoluble*
[$dmim^+$][Cl^-]	Insoluble*	ETAN	Insoluble*

*After 24 h at 90°C.

Table 1. Solubility (%wt) of SF in selected ILs at 90°C (heated in an oil bath). From Ref. [23] with permission of Wiley Online Library.

	Silk fibroin (SF)		Silk cocoon (SC)	
Solvent	**Solubility (%wt)**	**Time (min.)**	**Solubility (%wt)**	**Time (min.)**
[mim$^+$][Cl$^-$]	12.5 ± 0.1	4	12.5 ± 0.1	17
[emim$^+$][Cl$^-$]	23.0 ± 0.3	17	18.7 ± 0.6	67
[pmim$^+$][Cl$^-$]	15.2 ± 0.3	14	17.6 ± 0.1	27
[bmim$^+$][Cl$^-$]	12.7 ± 0.6	5	12.9 ± 0.4	24
[hmim$^+$][Cl$^-$]	10.9 ± 0.2	8	11.1 ± 0.3	20

Solubility is presented as the average value ± SD (standard deviation) (n = 3).

Table 2. Solubility and time required for dissolution of silk proteins, in selected ILs. From Ref. [23] with permission of Wiley Online Library.

Silk protein integrity in the SIL solutions was confirmed by sodium dodecyl sulfate-polyacrylamide gel electrophoresis (SDS-PAGE). It was found that the peptidic chain fragmentation that occurs when the classical dissolution methods are used is drastically reduced in the process with ILs and high-power ultrasound. In **Figure 6**, the molecular masses of the fragments of the SIL solutions may be observed, which are practically the same than that of the SF present in the silkworm gland [53].

The overall process of SFNs preparation from SIL solutions is summarized in **Figure 7**. The procedure is based on the method described previously by Zhang et al., with modifications [52].

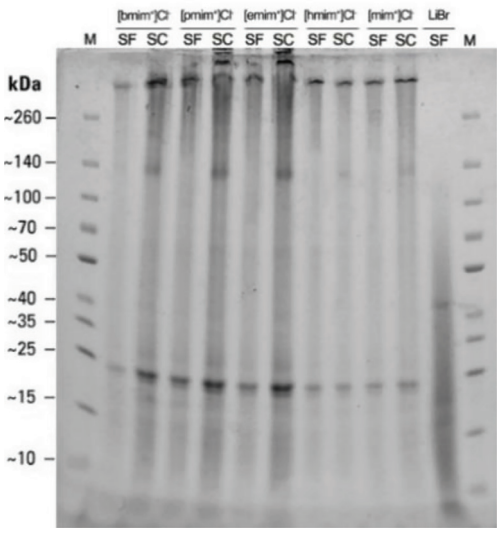

Figure 6. Sodium dodecyl sulfate-polyacrylamide gel electrophoresis of the protein components of silk fibroin (SF) and white silk cocoons (SC) after the use of high-power ultrasounds in the solutions SC/IL or SF/IL with ILs: [bmim$^+$][Cl$^-$], [pmim$^+$][Cl$^-$], [emim$^+$][Cl$^-$], [hmim$^+$][Cl$^-$] and [mim$^+$][Cl$^-$]. From Ref. [23] with permission of Wiley Online Library.

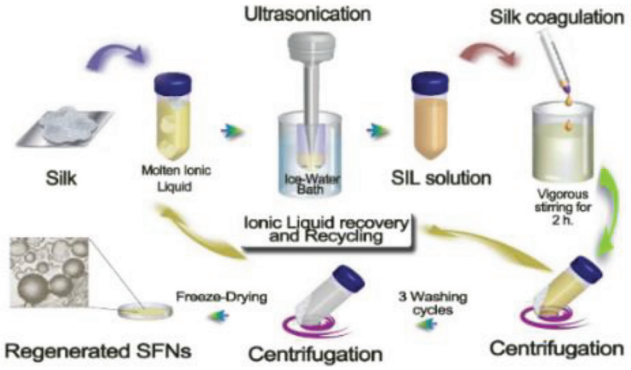

Figure 7. Scheme of the overall process of SF dissolution, using ILs and ultrasonication, and consequent SFNs preparation from SIL solutions. From Ref. [23] with permission of Wiley Online Library.

In brief, to the freshly prepared SIL solution, ultrapure water was added to reduce its viscosity, and the SIL solution was slowly dripped into 100 mL of vigorously stirred cold methanol. After a few drops, a milky-white suspension appeared and the suspension was stirred for 2 h. The particle suspension was recovered by centrifugation at 18,000 *g* for 15 min, at 4°C. The supernatant (free of particles) was removed and reserved for subsequent recycling of the IL. The white precipitate was subjected to successive rinses with fresh methanol and ultrapure water. After lyophilizing the particles for 72 h at 0.5 mbar and −55°C (Edwards Modulyo 4 K Freeze Dryer), SFNs were obtained in the form of a dry powder. A rotary evaporator at 80 mbar and 80°C was used to recover the IL from the methanolic and water fractions.

The liquid silk fibroin can be regenerated as nanoparticles by pouring SIL solution into an excess of a polar organic solvent. In this case, methanol was used for SF regeneration. When the IL is dissolved in methanol from the SIL solution, the SF changes from random coil and α-helix forms into anti-parallel β-sheet form by reconstitution of the hydrogen bonds network of the protein chains [52].

The particles were characterized by dynamic light scattering (DLS) and infrared spectroscopy (FTIR). The stability of the particles was tested in purified water at 25°C and in Dulbecco's Modified Eagle Medium (DMEM) (without Fetal Bovine Serum (FBS) supplementation) at 37°C. In MilliQ water at 25°C, the SFNs had an average size of 170–184 nm measured by DLS. The results indicate that the particles were slightly larger (183–341 nm) when dispersed in DMEM (see **Table 3**); these values are almost identical to those described previously in the corresponding study [52, 54].

In **Figure 8**, a comparative FTIR spectrum of [bmim$^+$][Cl$^-$], SFNs regenerated from SF/[bmim$^+$][Cl$^-$] solution and SFNs regenerated from classical $CaCl_2$/EtOH/H_2O solution, obtained using the classical Zhang's method [52] is presented. As can be observed, β-sheet is predominant in particles with peaks at 1230 (Amide III, C-H Stretching), 1516 (Amide II, N-H Bending), and 1626 cm^{-1} (Amide I, C=O Stretching), which are typical of the β-sheet conformation [27]. The SFN profiles were similar to those of SFNs obtained by methanol immersion of SF dissolved

	MilliQ water at 25°C			DMEM at 37°C		
Solvent used	**Diameter[a] (nm)**	**PdI[b]**	**Zpot[a] (mV)**	**Diameter[a] (nm)**	**PdI[b]**	**Zpot[a] (mV)**
$CaCl_2/EtOH/H_2O$	174 ± 2	0.121	−26.23 ± 0.59	183 ± 3	0.140	−12.02 ± 0.42
$[mim^+][Cl^-]$	177 ± 4	0.153	−27.15 ± 0.74	208 ± 4	0.115	−12.08 ± 1.50
$[emim^+][Cl^-]$	181 ± 3	0.230	−25.65 ± 0.90	341 ± 9	0.393	−12.00 ± 2.12
$[pmim^+][Cl^-]$	175 ± 4	0.129	−27.53 ± 0.66	211 ± 4	0.076	−12.22 ± 1.09
$[bmim^+][Cl^-]$	184 ± 5	0.212	−24.53 ± 1.42	235 ± 4	0.245	−12.24 ± 1.66
$[hmim^+][Cl^-]$	176 ± 3	0.140	−27.90 ± 0.82	200 ± 3	0.133	−11.28 ± 0.55

[a]Z-average ± SD (n = 5) and accumulation times = 100.
[b]Average value.

Table 3. Comparative values for the particle size (diameter), polydispersity (PdI), and zeta potential of classical SFNs [52] obtained from $CaCl_2/EtOH/H_2O$ solvent and SFNs produced from SIL solutions. From Ref. [23] with permission of Wiley Online Library.

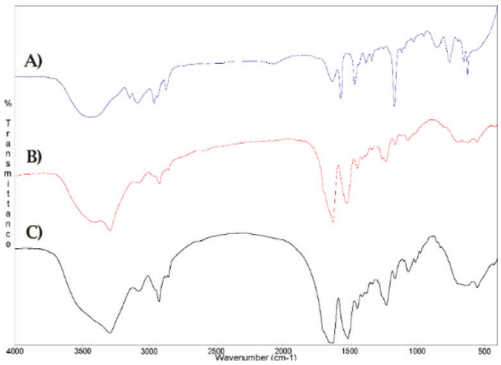

Figure 8. Comparative FTIR spectra of (A) only $[bmim^+][Cl^-]$; (B) SFNs regenerated from SF/$[bmim^+][Cl^-]$ solution; (C) SFNs regenerated from classical $CaCl_2/EtOH/H_2O$ solution [52]. From Ref. [23] with permission of Wiley Online Library.

in the Ajisawa solvent system [52, 55]. Characteristic signals of ILs (1572, 1465, and 1170 cm^{-1}) were absent in the recorded spectrum of SFNs obtained from $[bmim^+][Cl^-]$, indicating that the IL was efficiently washed out from the SFNs.

2.5.1. Synthesis of curcumin-loaded silk fibroin nanoparticles using ILs

Curcumin ((1*E*,6*E*)-1,7-bis(4-hydroxy-3-methoxyphenyl)hepta-1,6-diene-3,5-dione, **Figure 9**) is a hydrophobic polyphenol derived from turmeric: the rhizome of the herb *Curcuma longa* [56]. From the chemical point of view, curcumin is a bis-α,β-unsaturated β-diketone (also called diferuloylmethane) that shows keto-enol tautomerism, with a stable enol form in alkaline media and a predominant keto form in acidic and neutral solutions. Commercial curcumin is a mixture of curcuminoids (approximately, 77% diferuloylmethane, 18% demethoxycurcumin, and 5% bisdemethoxycurcumin) [57]. *C. longa* mainly grows in China and India although it can

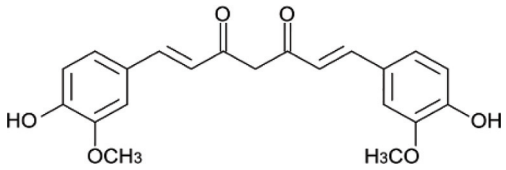

Figure 9. Chemical structure of curcumin [5].

also be present in the rest of the Asian continent and has been widely employed in Ayurvedic medicine for centuries [58]. Its most relevant pharmacological effects are its anti-inflammatory [59], anticancer [57], antioxidant [60], and antimicrobial [60] activities.

Although curcumin is safe, nontoxic, and well tolerated in animal and human studies, it cannot be administered to patients directly due to its poor solubility in water [56] (estimated value: 3.12 mg/L at 25°C [61]). In an attempt to enhance the therapeutic efficiency of curcumin, improvements in its bioavailability have been tried. Several nanocarriers such as solid lipid nanoparticles [62], natural [63] or synthetic [64] polymer nanoparticles, and inorganic nanoparticles [65] can be found in the study as examples of nanoplatforms for the intracellular delivery of curcumin. Recently, research interests focus on the use of biopolymers such as SF to encapsulate curcumin and other similar drugs [66]. By virtue of their small size, SFNs can penetrate thin capillaries, fostering the uptake of drugs by cells. In addition, these SFNs are potential targeted delivery systems because, for instance, they can deliver antitumor drugs to tumor cells. Several research groups have studied curcumin encapsulation in SFNs by different techniques [67, 68].

The authors [5] studied the synthesis of curcumin-loaded SFNs (Curc-SFNs) to improve on current methods, using IL (1-ethyl-3-methylimidazolium acetate, $[emim^+][CH_3COO^-]$) and high-power ultrasounds to dissolve the SF. The synthesis of Curc-SFNs developed in this chapter is a more scalable and continuous processing option than those already published in the study. The drug was loaded into the SFNs by physical adsorption, Curc-SFNs 1, and by coprecipitation, Curc-SFNs 2, in order to obtain Curc-SFNs.

For loading of curcumin by physical adsorption, 40 mL of a 1 mg/mL solution of curcumin in ethanol was used to resuspend 325 mg of SFNs obtained from an SF-IL solution. The suspension was ultrasonicated for 5 min and gently stirred at 30 rpm in a Tube Rotator for 24 h. Next, Curc-SFNs 1 were centrifuged for 15 min at 13,400 rpm. Finally, Curc-SFNs 1 were washed with water to eliminate the rest of ethanol. The drug loaded in the nanoparticles was indirectly determined by the measurement of the UV absorbance of curcumin at 421 nm in the centrifugation supernatants (ethanol and water) and in the initial curcumin solution.

To obtain Curc-SFNs 2 by coprecipitation, the drug was loaded in the nanoparticles throughout the synthesis step. In brief, an exact weighed amount of curcumin (25 mg) was dissolved in 3 mL of 0.1 M NaOH solution, and this solution was immediately dissolved in 5 g of a previously prepared SIL solution (10% wt.). The drug-SIL solution was heated to 60°C to reduce the viscosity of the mixture and sprayed with nitrogen onto 100 mL of gently stirred ethanol. The orange suspension was stirred for 2 h before being centrifuged at 13,400 rpm for

15 min, at 4°C. In this case, three washes with water were carried out to remove the IL. Lyophilization was carried out under the experimental conditions described earlier.

Drug loading content (DLC) and entrapment efficiency (EE) of Curc-SFNs 1 and Curc-SFNs 2 obtained were calculated according to the following expressions from the measurements of UV–Vis absorbance of curcumin:

$$\boldsymbol{DLC = \frac{weight\ of\ the\ drug\ in\ nanoparticles}{weight\ of\ the\ nanoparticles} \cdot 100} \quad (1)$$

$$EE = \frac{weight\ of\ the\ drug\ in\ nanoparticles}{weight\ of\ the\ feeding\ drugs} \cdot 100 \quad (2)$$

As can be seen in **Table 4**, DLC values in the physical adsorption assays were higher than in the coprecipitation experiments, probably due to the much higher initial curcumin/SF mass ratio in the physical adsorption experiments. Nevertheless, the EE values were about 50% for both types of nanoparticles. DLC and EE are in the same order or even higher than those found in the study [69, 70].

Furthemore, the mean hydrodynamic diameter (Z-average), the PdI, the zeta potential, and the electrophoretic mobility were measured by DLS. All measurements were performed in purified water at 25°C. The mean values of the measurements performed in triplicate are reported in **Table 5**. The results revealed that the Z-average of the SFNs was smaller than of the particles with curcumin, whereas the PdI values were similar and lower than 0.15 for all types of nanoparticles, resulting in size distributions practically monodisperse. The zeta potential of the nanoparticles with and without curcumin was highly negative and of the same order of magnitude, indicating their high colloidal stability and higher than the values found in

	Curc-SFNs 1[1]	**Curc-SFNs 2[1]**
DLC (%)	6.63 ± 0.09	2.47 ± 0.11
EE (%)	53.75 ± 0.81	48.84 ± 2.67

[1]Mean values ± SD (standard deviation) (n = 3).

Table 4. Drug loading and encapsulation efficiency of the Cur-SFNs [5].

	Zeta potential (mV)	**Z-average (nm)**	**Electrophoretic mobility (μmcm/Vs)**	**PdI**
Curc-SFNs 1	−42.9 ± 2.8	166.0 ± 0.1	−3.362 ± 0.264	0.114 ± 0.003
Curc-SFNs 2	−45.9 ± 5.0	171.2 ± 2.6	−3.504 ± 0.348	0.106 ± 0.017
SFNs	−41.3 ± 0.6	157.9 ± 1.5	−3.396 ± 0.146	0.132 ± 0.011

Mean values ± SD (standard deviation).

Table 5. Physical characterization of the Curc-SFNs. From Ref. [5] with permission of MDPI.

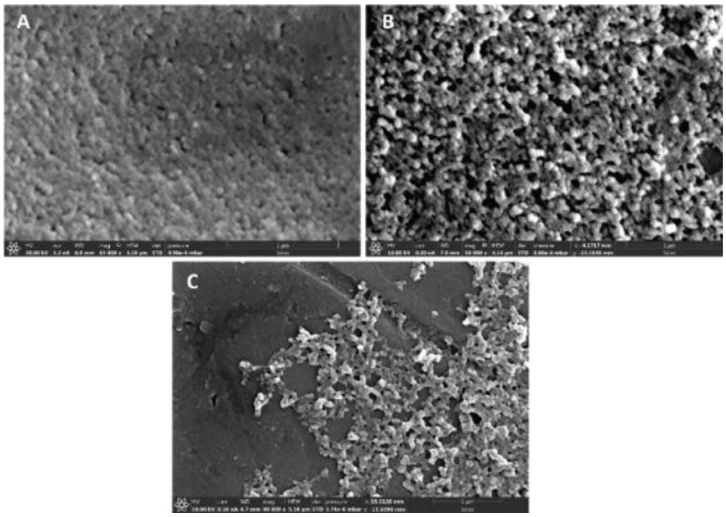

Figure 10. FESEM pictures of (a) SFNs, (b) Curc-SFNs 1, and (c) Curc-SFNs 2 [5].

previous studies which synthesize SFNs by classical methods [52, 70], which reflects the improvement in stability of the SFNs and hence of the Curc-SFNs obtained with this new procedure.

The morphology of the nanoparticles was examined by field emission scanning electron microscopy (FESEM). As can be observed in **Figure 10**, SFNs and Curc-SFNs 1 present nanospherical morphology. However, Curc-SFNs 2 has elongated shape. FESEM micrographs showed smaller sizes than the DLS measurements. This could be due to the swelling of the nanoparticles in the water solution in DLS measurements. This difference has also been observed in previous works [52, 69].

The Curc-SFNs obtained in this work enhanced the antitumor activity of curcumin toward the two different tumor cell lines studied (hepatocellular carcinoma, Hep3B and human neuroblastoma, Kelly Cells), while the viability of the healthy cells (human bone marrow-derived mesenchymal stem cells, hBMSCs) did not decrease. This broadens the possibility of using these SFNs, which have been synthesized by an industrial process, as future systems for other drugs of hydrophilic or hydrophobic nature, such as curcumin.

3. Conclusions

ILs are excellent candidates to participate in the synthesis of biopolymeric nanoparticles mainly because they can dissolve biopolymers due to their design flexibility by combining different cation and anion and their green solvent properties such as non-volatility, non-flammability, and recyclability. Different biopolymers, such as cellulose, xylan, starch, chitosan, keratin, and

silk fibroin, were used to obtain nanoparticles in processes involving ILs. We synthetized SFNs by a new methodology using high-power ultrasounds to enhance the dissolution of the protein in the IL. From SIL solutions, SFNs were obtained by regeneration of the SF in an organic polar solvent, and SFNs showed a high degree of β-sheet, similar to that of the SF native fibers. In this way, large amounts of silk can be turned into biomaterials directly from the dissolved SIL solution, for use in a wide range of applications. Focusing on the biomedical application, Curc-SFNs were successfully synthesized by two environmentally friendly procedures using ILs and high-power ultrasound to dissolve the SF. High DLC and EE values were obtained in both cases compared with those in the study. The SFNs and the Curc-SFNs obtained showed a narrow size distribution, with a hydrodynamic diameter of <175 nm, and high zeta potential (in absolute terms), which make them excellent nanocarriers for use in therapeutic treatments.

Acknowledgements

This work has been partially supported from the European Commission (FEDER/ERDF) and the Spanish MINECO (Ref. CTQ2014-57467-R and Ref. CTQ2017-87708-R) and the programme of support to the research of the Seneca Foundation of Science and Technology of Murcia, Spain (Ref. 19499/PI/14). The research contract of Dr. A. Abel Lozano-Pérez was partially supported (80%) by the ERDF/FEDER Operative Programme of the Region of Murcia (Project No. 14-20-01).

Conflict of interest

The authors declare no conflict of interest.

Author details

Mercedes G. Montalbán[1], Guzmán Carissimi[2], A. Abel Lozano-Pérez[3], José Luis Cenis[3], Jeannine M. Coburn[4,5], David L. Kaplan[4] and Gloria Víllora[2]*

*Address all correspondence to: gvillora@um.es

1 Department of Chemical Engineering, University of Alicante, Alicante, Spain

2 Department of Chemical Engineering, Faculty of Chemistry, Regional Campus of International Excellence "Campus Mare Nostrum", University of Murcia, Murcia, Spain

3 Department of Biotechnology, Instituto Murciano de Investigación y Desarrollo Agrario y Alimentario (IMIDA), La Alberca (Murcia), Spain

4 Department of Biomedical Engineering, Tufts University, Medford, MA, USA

5 Department of Biomedical Engineering, Worcester Polytechnic Institute, Worcester, MA, USA

References

[1] Lee SH, Miyauchi M, Dordick JS, Linhardt RJ. Preparation of biopolymer-based materials using ionic liquids for the biomedical application. In: Malhotra SV, editor. Ionic Liquid Applications: Pharmaceuticals, Therapeutics, and Biotechnology. 1st ed. ACS Symposium Series, Washington D.C. (USA): ACS Publications; 2010. pp. 115-134. DOI: 10.1021/bk-2010-1038.ch010

[2] Nitta SK, Numata K. Biopolymer-based nanoparticles for drug/gene delivery and tissue engineering. International Journal of Molecular Sciences. 2013;**14**:1629-1654. DOI: 10.3390/ijms14011629

[3] Yih TC, Al-Fandi M. Engineered nanoparticles as precise drug delivery systems. Journal of Cellular Biochemistry. 2006;**97**:1184-1190. DOI: 10.1002/jcb.20796

[4] Lozano-Pérez AA, Rivero HC, Pérez Hernández MC, Pagán A, Montalbán MG, Víllora G, Cenis JL. Silk fibroin nanoparticles: Efficient vehicles for the natural antioxidant quercetin. International Journal of Pharmaceutics. 2017;**518**:11-19. DOI: 10.1016/j.ijpharm.2016.12.046

[5] Montalbán MG, Coburn JM, Lozano-Pérez AA, Cenis JL, Víllora G, Kaplan DL. Production of curcumin-loaded silk fibroin nanoparticles for cancer therapy. Nanomaterials. 2018;**8**:1-18. DOI: 10.3390/nano8020126

[6] Gómez-Murcia V, Montalbán MG, Gómez-Fernández JC, Almela P. Development of poly (lactide-co-glicolide) nanoparticles incorporating morphine hydrochloride to prolong its circulation in blood. Current Pharmaceutical Design. 2017;**23**:2015-2025. DOI: 10.2174/1381612826661612011526 04

[7] Ahmed TA, El-Say KM. Development of alginate-reinforced chitosan nanoparticles utilizing W/O nanoemulsification/internal crosslinking technique for transdermal delivery of rabeprazole. Life Sciences. 2014;**110**:35-43. DOI: 10.1016/J.LFS.2014.06.019

[8] Damgé C, Maincent P, Ubrich N. Oral delivery of insulin associated to polymeric nanoparticles in diabetic rats. Journal of Controlled Release. 2007;**117**:163-170. DOI: 10.1016/J.JCONREL.2006.10.023

[9] Werfel T, Duvall C. Polymeric nanoparticles for gene delivery. In: Narain R, editor. Polymers and Nanomaterials for Gene Therapy. 1st ed. Amsterdam (Netherlands): Elsevier; 2016. pp. 147-188. DOI: 10.1016/B978-0-08-100520-0.00007-2

[10] Yang Y-Y, Wang Y, Powell R, Chan P. Polymeric core-shell nanoparticles for therapeutics. Clinical and Experimental Pharmacology & Physiology. 2006;**33**:557-562. DOI: 10.1111/j.1440-1681.2006.04408.x

[11] Elzoghby AO, Samy WM, Elgindy NA. Protein-based nanocarriers as promising drug and gene delivery systems. Journal of Controlled Release. 2012;**161**:38-49. DOI: 10.1016/J.JCONREL.2012.04.036

[12] Mohammad Fauzi AH, Amin NAS. An overview of ionic liquids as solvents in biodiesel synthesis. Renewable and Sustainable Energy Reviews. 2012;**16**:5770-5786. DOI: 10.1016/j.rser.2012.06.022

[13] Keskin S, Kayrak-Talay D, Akman U, Hortaçsu Ö. A review of ionic liquids towards supercritical fluid applications. Journal of Supercritical Fluids. 2007;**43**:150-180. DOI: 10.1016/j.supflu.2007.05.013

[14] Montalbán MG, Hidalgo JM, Collado-González M, Díaz Baños FG, Víllora G. Assessing chemical toxicity of ionic liquids on Vibrio fischeri: Correlation with structure and composition. Chemosphere. 2016;**155**:405-414. DOI: 10.1016/j.chemosphere.2016.04.042

[15] Mudring A-V, Alammar T, Bäcker T, Richter K. Nanoparticle synthesis in ionic liquids. In: Plechkova NV, Rogers RD, Seddon KR, editors. Ionic Liquids: From Knowledge to Application. ACS Symposium Series, Washington D.C. (USA): ACS Publications; 2010. pp. 177-188. DOI: 10.1021/bk-2009-1030.ch012

[16] Anastas PT, Warner JC. Green Chemistry: Theory and Practice. 1st ed. New York: Oxford University Press; 1998. 148 p

[17] Torimoto T, Okazaki K, Kiyama T, Hirahara K, Tanaka N, Kuwabata S. Sputter deposition onto ionic liquids: Simple and clean synthesis of highly dispersed ultrafine metal nanoparticles. Applied Physics Letters. 2006;**89**:243117. DOI: 10.1063/1.2404975

[18] Zhu Y-J, Wang W-W, Qi R-J, Hu X-L. Microwave-assisted synthesis of single-crystalline tellurium nanorods and nanowires in ionic liquids. Angewandte Chemie International Edition. 2004;**43**:1410-1414. DOI: 10.1002/anie.200353101

[19] Bühler G, Feldmann C. Microwave-assisted synthesis of luminescent LaPO4:Ce,Tb nanocrystals in ionic liquids. Angewandte Chemie International Edition. 2006;**45**:4864-4867. DOI: 10.1002/anie.200600244

[20] Swatloski RP, Spear SK, Holbrey JD, Rogers RD. Dissolution of cellulose with ionic liquids. Journal of the American Chemical Society. 2002;**124**:4974-4975. DOI: 10.1021/JA025790M

[21] Phillips DM, Drummy LF, Conrady DG, Fox DM, Naik RR, Stone MO, Trulove PC, De Long HC, Mantz RA. Dissolution and regeneration of *Bombyx mori* silk fibroin using ionic liquids. Journal of the American Chemical Society. 2004;**126**:14350-14351. DOI: 10.1021/JA046079F

[22] Flannigan DJ, Hopkins SD, Suslick KS. Sonochemistry and sonoluminescence in ionic liquids, molten salts, and concentrated electrolyte solutions. Journal of Organometallic Chemistry. 2005;**690**:3513-3517. DOI: 10.1016/J.JORGANCHEM.2005.04.024

[23] Lozano-Pérez AA, Montalbán MG, Aznar-Cervantes SD, Cragnolini F, Cenis JL, Víllora G. Production of silk fibroin nanoparticles using ionic liquids and high-power ultrasounds. Journal of Applied Polymer Science. 2015;**132**:1-8. DOI: 10.1002/app.41702

[24] Schlufter K, Schmauder HP, Dorn S, Heinze T. Efficient homogeneous chemical modification of bacterial cellulose in the ionic liquid 1-N-butyl-3-methylimidazolium chloride. Macromolecular Rapid Communications. 2006;**27**:1670-1676. DOI: 10.1002/marc.200600463

[25] Gautam SP, Bundela PS, Pandey AK, Awasthi MK, Sarsaiya S. A review on systematic study of cellulose. Journal of Applied and Natural Science. 2010;**2**:330-343

[26] Ashby MF, Gibson LJ, Wegst U, Olive R. The mechanical properties of natural materials. I. Material property charts. Proceedings of the Royal Society A: Mathematical, Physical and Engineering Sciences. 1995;**450**:123-140. DOI: 10.1098/rspa.1995.0075

[27] Han J, Zhou C, French AD, Han G, Wu Q. Characterization of cellulose II nanoparticles regenerated from 1-butyl-3-methylimidazolium chloride. Carbohydrate Polymers. 2013; **94**:773-781. DOI: 10.1016/j.carbpol.2013.02.003

[28] Köhler S, Liebert T, Heinze T. Interactions of ionic liquids with polysaccharides. VI. Pure cellulose nanoparticles from trimethylsilyl cellulose synthesized in ionic liquids. Journal of Polymer Science Part A: Polymer Chemistry. 2008;**46**:4070-4080. DOI: 10.1002/pola.22749

[29] Swatloski R, Holbrey J, Weston JL, Rogers RD. Preparation of magnetic cellulose composites using ionic liquids. Chimica Oggi. 2006;**24**:31

[30] Ebringerová A, Heinze T. Xylan and xylan derivatives–Biopolymers with valuable properties, 1: Naturally occurring xylans structures, isolation procedures and properties. Macromolecular Rapid Communications. 2000;**21**:542-556. DOI: 10.1002/1521-3927(20000601)21:9<542::AID-MARC542>3.0.CO;2-7

[31] Gericke M, Gabriel L, Geitel K, Benndorf S, Trivedi P, Fardim P, Heinze T. Synthesis of xylan carbonates—An approach towards reactive polysaccharide derivatives showing self-assembling into nanoparticles. Carbohydrate Polymers. 2018;**193**:45-53. DOI: 10.1016/j.carbpol.2018.03.083

[32] Petzold-Welcke K, Schwikal K, Daus S, Heinze T. Xylan derivatives and their application potential—Mini-review of own results. Carbohydrate Polymers. 2014;**100**:80-88. DOI: 10.1016/j.carbpol.2012.11.052

[33] Ross AS. Starch in foods. In: Food Carbohydrate. Chemistry. 1st ed. New Jersey (USA): Wiley Online Library; 2013. pp. 107-133. DOI: 10.1002/9781118688496.ch7

[34] Pérez S, Baldwin PM, Gallant DJ. Structural Features of Starch Granules I. 3rd ed. Amsterdam (Netherlands): Elsevier; 2009. DOI: 10.1016/B978-0-12-746275-2.00005-7

[35] Jl J. Structural Features of Starch Granules II. 3rd ed. Amsterdam (Netherlands): Elsevier; 2009. DOI: 10.1016/B978-0-12-746275-2.00006-9

[36] Zhou G, Luo Z, Fu X. Preparation and characterization of starch nanoparticles in ionic liquid-in-oil microemulsions system. Industrial Crops and Products. 2014;**52**:105-110. DOI: 10.1016/j.indcrop.2013.10.019

[37] Zhou G, Luo Z, Fu X. Preparation of starch nanoparticles in a water-in-ionic liquid microemulsion system and their drug loading and releasing properties. Journal of Agricultural and Food Chemistry. 2014;**62**:8214-8220. DOI: 10.1021/jf5018725

[38] Zhigang L, Linrong S, Meina Z. Preparation of starch nanoparticles in a new ionic liquid-in-oil micro- emulsion. Journal of Formulation Science & Bioavailability. 2017;**1**:1-8. DOI: 10.4172/2577-0543.1000116

[39] Wang X, Cheng J, Ji G, Peng X, Luo Z. Starch nanoparticles prepared in a two ionic liquid based microemulsion system and their drug loading and release properties. RSC Advances. 2016;**6**:4751-4757. DOI: 10.1039/C5RA24495A

[40] Ji G, Luo Z, Xiao Z, Peng X. Synthesis of starch nanoparticles in a novel microemulsion with two ILs substituting two phases. Journal of Materials Science. 2016;**51**:7085-7092. DOI: 10.1007/s10853-016-9952-1

[41] Divya K, Jisha MS. Chitosan nanoparticles preparation and applications. Environmental Chemistry Letters. 2018;**16**:101-112. DOI: 10.1007/s10311-017-0670-y

[42] Torzsas TL, Kendall CWC, Sugano M, Iwamoto Y, Rao AV. The influence of high and low molecular weight chitosan on colonic cell proliferation and aberrant crypt foci development in CF1 mice. Food and Chemical Toxicology. 1996;**34**:73-77. DOI: 10.1016/0278-6915(95)00083-6

[43] Bharmoria P, Singh T, Kumar A. Complexation of chitosan with surfactant like ionic liquids: Molecular interactions and preparation of chitosan nanoparticles. Journal of Colloid and Interface Science. 2013;**407**:361-369. DOI: 10.1016/J.JCIS.2013.06.032

[44] Al Kobiasi M, Chua BY, Tonkin D, Jackson DC, Mainwaring. Control of size dispersity of chitosan biopolymer microparticles and nanoparticles to influence vaccine trafficking and cell uptake. Journal of Biomedical Materials Research Part A. 2012;**100**:1859-1867. DOI: 10.1002/jbm.a.34153

[45] Sonia TA, Sharma CP. An overview of natural polymers for oral insulin delivery. Drug Discovery Today. 2012;**17**:784-792. DOI: 10.1016/j.drudis.2012.03.019

[46] Omenetto FG, Kaplan DL. New opportunities for an ancient material. Science. 2010;**329**:528-531. DOI: 10.1126/science.1188936

[47] Hofmann S, Wong Po Foo CT, Rossetti F, Textor M, Vunjak-Novakovic G, Kaplan DL, Merkle HP, Meinel L. Silk fibroin as an organic polymer for controlled drug delivery. Journal of Controlled Release. 2006;**111**:219-227. DOI: 10.1016/j.jconrel.2005.12.009

[48] Ajisawa A. Dissolution aqueous of silk fibroin with calcium chloride/ethanol solution. The Journal of Sericultural Science of Japan. 1997;**67**:91-94

[49] Asakura T, Watanabe Y, Uchida A, Minagawa H. NMR of silk fibroin. Carbon-13 NMR study of the chain dynamics and solution structure of *Bombyx mori* silk fibroin. Macromolecules. 1984;**17**:1075-1081. DOI: 10.1021/ma00135a017

[50] Rockwood DN, Preda RC, Yücel T, Wang X, Lovett ML, Kaplan DL. Materials fabrication from *Bombyx mori* silk fibroin. Nature Protocols. 2011;**6**:1612-1631. DOI: 10.1038/nprot.2011.379

[51] Wang Q, Yang Y, Chen X, Shao Z. Investigation of rheological properties and conformation of silk fibroin in the solution of AmimCl. Biomacromolecules. 2012;**13**:1875-1881. DOI: 10.1021/bm300387z

[52] Zhang Y-Q, Shen W-D, Xiang R-L, Zhuge L-J, Gao W-J, Wang W-B. Formation of silk fibroin nanoparticles in water-miscible organic solvent and their characterization. Journal of Nanoparticle Research. 2007;**9**:885-900. DOI: 10.1007/s11051-006-9162-x

[53] Yamada H, Nakao H, Takasu Y, Tsubouchi K. Preparation of undegraded native molecular fibroin solution from silkworm cocoons. Materials Science and Engineering: C. 2001;**14**: 41-46. DOI: 10.1016/S0928-4931(01)00207-7

[54] Kundu J, Chung Y-I, Kim YH, Tae G, Kundu SC. Silk fibroin nanoparticles for cellular uptake and control release. International Journal of Pharmaceutics. 2010;**388**:242-250. DOI: 10.1016/j.ijpharm.2009.12.052

[55] Cao Z, Chen X, Yao J, Huang L, Shao Z. The preparation of regenerated silk fibroin microspheres. Soft Matter. 2007;**3**:910-915. DOI: 10.1039/b703139d

[56] Bhawana BRK, Buttar HS, Jain VK, Jain N. Curcumin nanoparticles: Preparation, characterization, and antimicrobial study. Journal of Agricultural and Food Chemistry. 2011;**59**: 2056-2061. DOI: 10.1021/jf104402t

[57] Anand P, Sundaram C, Jhurani S, Kunnumakkara AB, Aggarwal BB. Curcumin and cancer: An "old-age" disease with an "age-old" solution. Cancer Letters. 2008;**267**:133-164. DOI: 10.1016/j.canlet.2008.03.025

[58] Wilken R, Veena MS, Wang MB, Srivatsan ES. Curcumin: A review of anti-cancer properties and therapeutic activity in head and neck squamous cell carcinoma. Molecular Cancer. 2011;**10**:1-19. DOI: 10.1186/1476-4598-10-12

[59] Kohli K, Ali J, Ansari MJ, Raheman Z. Curcumin : A natural antiinflammatory agent. Indian Journal of Pharmacology. 2005;**37**:141-147. DOI: 10.4103/0253-7613.16209

[60] Mahmood K, Zia KM, Zuber M, Salman M, Anjum MN. Recent developments in curcumin and curcumin based polymeric materials for biomedical applications: A review. International Journal of Biological Macromolecules. 2015;**81**:877-890. DOI: 10.1016/j.ijbiomac.2015.09.026

[61] US EPA, Estimation Program Interface (EPI) Suite. Ver. 4.1. Nov. 2012

[62] Hassan HA, Florentin M, Sandrine BNI, Pierrick D, Jordane J, Michel L. Shea butter solid nanoparticles for curcumin encapsulation: Influence of nanoparticles size on drug loading. European Journal of Lipid Science and Technology. 2015;**118**:1168-1178. DOI: 10.1002/ejlt.201500348

[63] Anitha A, Maya S, Deepa N, Chennazhi KP, Nair SV, Tamura H, Jayakumar R. Efficient water soluble O-carboxymethyl chitosan nanocarrier for the delivery of curcumin to cancer cells. Carbohydrate Polymers. 2011;**83**:452-461. DOI: 10.1016/j.carbpol.2010.08.008

[64] Akl MA, Kartal-Hodzic A, Oksanen T, Ismael HR, Afouna MM, Yliperttula M, Samy AM, Viitala T. Factorial design formulation optimization and in vitro characterization of curcumin-loaded PLGA nanoparticles for colon delivery. Journal of Drug Delivery Science and Technology. 2016;**32**:10-20. DOI: 10.1016/j.jddst.2016.01.007

[65] Bhandari R, Gupta P, Dziubla T, Hilt JZ. Single step synthesis, characterization and applications of curcumin functionalized iron oxide magnetic nanoparticles. Materials Science and Engineering: C. 2016;**67**:59-64. DOI: 10.1016/j.msec.2016.04.093

[66] Hu K, Huang X, Gao Y, Huang X, Xiao H, McClements DJ. Core-shell biopolymer nanoparticle delivery systems: Synthesis and characterization of curcumin fortified zein-pectin nanoparticles. Food Chemistry. 2015;**182**:275-281. DOI: 10.1016/j.foodchem.2015.03.009

[67] Xie M-B, Li Y, Zhao Z, Chen A-Z, Li J-S, Hu J-Y, Li G, Li Z. Solubility enhancement of curcumin via supercritical CO_2 based silk fibroin carrier. Journal of Supercritical Fluids. 2015;**103**:1-9. DOI: 10.1016/j.supflu.2015.04.021

[68] Song W, Muthana M, Mukherjee J, Falconer RJ, Biggs CA, Zhao X. Magnetic-silk core–Shell nanoparticles as potential carriers for targeted delivery of curcumin into human breast cancer cells. ACS Biomaterials Science & Engineering. 2017;**3**:1027-1038. DOI: 10.1021/acsbiomaterials.7b00153

[69] Xiao L, Lu G, Lu Q, Kaplan DL. Direct formation of silk nanoparticles for drug delivery. ACS Biomaterials Science & Engineering. 2016;**2**:2050-2057. DOI: 10.1021/acsbiomaterials.6b00457

[70] Tian Y, Jiang X, Chen X, Shao Z, Yang W. Doxorubicin-loaded magnetic silk fibroin nanoparticles for targeted therapy of multidrug-resistant cancer. Advanced Materials. 2014;**26**:7393-7398. DOI: 10.1002/adma.201403562